SEPTEMBER 26, 2019

PARAMETRIC SENSITIVITY OF THE VARSKIN DOSIMETRY MODELS

L. Anspach, C. Mangini, and D. Hamby
Renaissance Code Development, LLC

U.S.NRC
United States Nuclear Regulatory Commission
Protecting People and the Environment

Table of Contents

1 Introduction

VARSKIN is a deterministic dosimetry tool used by the NRC and licensees to approximate the shallow radiation dose to skin from radioactive contamination directly on the skin or on top of clothing. As a method to demonstrate compliance with 10 CFR 20.1201(c), VARSKIN can be used to calculate dose to skin over a contiguous 10 cm^2 of tissue at a depth of 7 mg/cm^2. Users develop the exposure scenario by choosing from a variety of source geometries, dose-averaging dimensions, radionuclide materials and activities, time estimations, and cover constituents. VARSKIN has been shown to be a very good estimator of shallow skin dose with simple geometric exposure characterizations (Anspach and Hamby 2017; Dubeau et al. 2018; Hamby et a. 2018).

The dosimetry models of VARSKIN were developed from first principles and then confirmed or refined based on the results of stochastic simulations using radiation transport codes. In these stochastic simulations, the uncertainty (i.e., statistical error) in each run was less than 5%, with most data having errors less than 1% (Mangini 2012). The pedigree from which VARSKIN was confirmed is quite precise.

VARSKIN itself does not perform stochastic simulations; therefore, statistical errors do not exist with its dose estimates. Deterministic uncertainty, however, is present with every dose prediction and is different than statistical error in that the uncertainties related to VARSKIN dose estimates are the result of imperfections of the deterministic models or mischaracterization of the exposure scenario by the user. As much as possible, deterministic modeling imperfections are addressed in the code itself by continuous evaluation of results and appropriate modifications to dose models. The primary dose uncertainty lies within the scenario and how it is defined to execute VARSKIN. Therefore, the importance of this assessment lies in determining which input parameters have the most influence on the result (skin dose), i.e., a *sensitivity analysis*. In this document, therefore, we analyze the influence of exposure mischaracterization on shallow skin dosimetry and provide the reader with an assessment of the VARSKIN parameters of greatest importance.

2 Sources of Deterministic Sensitivity

Generally, the first thing the user must do prior to executing VARSKIN is to estimate the conditions under which the skin exposure took place. The user must consider what features best characterize the radiological contamination, where on the body it was located, and how long it was there. When trying to estimate the exposure scenario, the user specifies several parameters necessary to calculate dose, including those related to:

- source nuclide and activity;
- source geometry;
- skin dose averaging dimensions (2D or 3D);
- exposure time;
- source composition;
- cover materials (if any); and
- presence of an airgap (if any).

Regardless of dosimetry method (VARKSIN, MCNP, EGSnrc, etc.), dose estimates are only as good as the information at hand (hence the well-known phrase, "*garbage in, garbage out*"). Because practical constraints on time and cost typically limit the characterization process and development of inputs, bounding the exposure with multiple scenarios describing potential variability allows for a range of possible doses to be generated. In some cases, an initial point estimate is obtained from a conservative calculation to quickly assess radiological safety implications and justify needs for obtaining additional information and performing more realistic dose calculations. An example is presented to illustrate these points.

Example. *A lab technician spills a 5 mL solution of rhenium-186, with an activity concentration of 0.2 MBq/mL, over what appears to be a 50 cm² area on her lab coat. A similar but generic lab coat is described as having a thickness of 0.4 mm and a density of 0.9 g/cm³. The employee estimates her exposure at 4.5 hours. What is her estimated shallow skin dose, which parameters are most important in that determination, and what is the uncertainty of the estimate?*

Solution. To bound the employee's estimated dose, i.e., to provide an estimate of uncertainty in the dose prediction, the radiation safety technician analyzes what is known and what is assumed about the exposure. She "knows" the following: (1) some level of activity of ^{186}Rh was spilled on a technician's lab coat; (2) the coat can be described by its thickness and density; (3) the size of the source can be approximated; and (4) the activity exposed the technician's skin

for some length of time. There is obviously no detail in what she knows, therefore, in a conservative fashion (to realistically maximize the dose estimate) the technician "assumes" the following: (1) 5 mL of 0.2 MBq/mL (1 MBq) was spilled on the coat; (2) the coat is 0.4 cm thick with a density of 0.9 g/cm^3 (the coat is sometimes a cover and sometimes integrated with the source); (3) the activity spread uniformly into a circular area of 50 cm^2 on the coat; (4) the activity was present for 4.5 hours; and (5) an air-gap does not exist.

After considering areas of potential uncertainty in the exposure scenario, she contemplates the following three scenarios of source geometry based on what is known/assumed about the activity configuration:

> Scenario #1: the source (known to be 1 MBq of ^{186}Rh) is a point directly on the employee's skin (this will maximize the dose estimate);
>
> Scenario #2: the source is a 2-dimensional disk with a cross-sectional area of 50 cm^2 resting on top of the employee's lab coat (this will account for lateral spreading of the source; the lab coat is a 'cover' in this scenario); and
>
> Scenario #3: the source is in solution and is absorbed into the lab coat (i.e., the coat is the source), forming a cylindrical geometry with a cross-sectional area of 50 cm^2 and a thickness of 0.4 cm (this geometry is most realistic).

When the technician executes VARSKIN for these three different scenarios, the difference in dose estimates will be due solely to how the exposure scenario was defined. This difference, or "scenario uncertainty", will typically dominate any other parametric uncertainties that we might examine. If the scenario is modeled precisely, we would expect very little scenario uncertainty. But, if several assumptions went into scenario development, we would expect to see uncertainties as a result.

Looking at the dose estimates for the three scenarios, we see that the point source (scenario #1) provides the highest dose (708 mGy) because all activity is concentrated at one point; we generally expect that the point geometry provides the upper-bound dose estimate. The 2D disk scenario (#2) results in a dose (0.0542 mGy) that is a factor of 13,000 lower than the point-source estimate due to spreading of the source and due to the entire thickness of the lab coat acting as a very effective shield for the electrons emitted by ^{186}Rh; this estimate provides a lower-bound dose. The third scenario is one where the liquid source is imbedded in the lab coat and that dose (18.7 mGy) is about 38 times lower than the point estimate; this scenario is expected to provide the best

dose estimate as it contains the most realism (but, again, given that all other assumptions are correct).

Therefore, what is evident in the above example is that seemingly small variations in scenario can result in huge differences in dose estimates, hence very large uncertainties (4 orders of magnitude in this case) and a showing of how sensitive dose estimates can be to changes in various input parameter values. The exposure scenario itself is probably the greatest source of uncertainty in all VARSKIN executions. What the reader might notice is that exposure time, for example, is not varied; if this parameter is varied, even more uncertainty is produced. There are certain parameters that describe the exposure that are direct multipliers driving the dose estimate. For example, an assumed exposure time of 2 hours will result in a dose estimate that is twice that of an exposure that really lasted only 1 hour, a 100% uncertainty.

Other parameters introduce zero uncertainty to the dose estimate. The skin averaging area, for example, is mandated by regulation (10 cm^2), so there is no uncertainty associated with that parameter. Input uncertainty associated with exposure time and source activity, however, is fully propagated through the models to the dose estimate, i.e., a 50% uncertainty in activity results in a 50% uncertainty in the dose estimate (assuming no other uncertainties). Photon and electron emission characteristics from various radionuclides originate from ICRP 38 or ICRP 107 and are assumed to be "correct".

As explained in the next chapter, the remainder of this report examines the sensitivity of skin dose related to parameter inputs that describe volumetric sources, density and thickness of cover materials, thickness of any airgap that might be present, and the influence of cross-sectional area of two-dimensional disk sources. In those analyses, conclusions are drawn as to how much impact is expected in dose estimate outputs following input parametric variability.

3 Parametric Limits

To operate VARSKIN, the user is required to enter numeric values for several inputs describing details of the skin exposure. Most inputs have default settings, and all have options for the use of different units. Some input parameters pose a direct impact on the result (e.g., twice the exposure time results in twice the dose), while others may influence the dose estimate in a less obvious fashion.

The three parameters of (1) exposure time, (2) source activity, and (3) distributed activity are direct propagators of uncertainty. As described, the uncertainty in these parameters will propagate completely and fully through the model to dose. The three inputs of (1) volume averaging depth, (2) skin averaging area, and (3) skin thickness (depth) are without parametric uncertainty because they are defined by regulation (e.g., dose averaged over 10 cm^2 at a depth of 7 mg/cm^2) and dose is calculated at that precise depth and averaging area.

The remaining parameters (airgap thickness, cover thickness, cover density, source area, source diameter, source thickness, source density, and X- and Y-side lengths) are those with parametric uncertainty, and therefore the focus of this report. The parameters of source diameter, thickness, and X- and Y-lengths for volumetric sources have been combined such that we examine the sensitivity of "source volume". The offset particle distance is only invoked in the point-source photon dosimetry model, to be used in the event of multiple hot particles within a few centimeters of one another. The probability of this occurrence is small, and since this model only applies to photon/point emissions, we will not estimate dose sensitivity to that parameter.

The reader can see that most of the sensitivity lies in the direct multipliers of activity and exposure time. The dose estimate will likely be most influenced by the characterization of those two parameters. If, however, those values are well known, the influence of source material, cover material, and airgap provide the next level of importance. Again, these parameters are the focus of what follows.

4 Methodology

As with any deterministic model, it is recommended that bounding dose estimates be determined to account for unknown or uncertain exposure conditions. As such, the following *sensitivity analysis* was conducted to demonstrate how dose varies with user input, i.e., a demonstration of output (the dose estimate) sensitivity to input parameterization. Most of this assessment focuses on the characterization of volumetric sources and cover materials. That characterization is especially important for small volumetric sources as accurate dimensional measurements may be difficult to approximate. Rough estimates of material dimensions, constituency, etc. can lead to significant discrepancies between the predicted and actual interaction processes such as backscatter, energy self-absorption, and charged particle equilibrium, thereby greatly affecting the dose estimate.

To exemplify the effects of input uncertainties, a variety of scenarios were examined to demonstrate the parametric sensitivity of both the electron and photon dose models. This includes an analysis of dose for each source geometry with changing source density, volume (or area), and cover material definitions (density and thickness).

While the intended use of VARSKIN is to calculate dose from particle emissions of user-selected radionuclides, we have chosen to demonstrate the effects of user input on the dose estimates as a function of monoenergetic electrons and photons. Consistent with 10 CFR 20.1201(c), all dosimetry calculations herein are averaged over a 10 cm^2 area at the precise depth of 7 mg/cm^2 and use ICRP 38 (or ICRP 107) decay data. A dose-averaging feature is available for volumes of tissue beneath the surface of skin, but this report does not evaluate uncertainties related to volume averaging.

Source volumes were chosen to sample over a large range of source dimensions that might have the greatest impact on skin dose. Unless the source is examined with a high-power microscope, dimensions on the order of microns are too small for an individual to determine and dose can be approximated by assuming a point source. Even in the event where dimensions are determined using high precision tools, the VARSKIN estimates approach that of a point source at these small dimensions. Generally, dimensions less than a micron are insignificant to the dose estimate therefore representing a lower limit on distance/thickness. Dimensions greater than this value may also be insignificant depending on the energy of electrons or photons being emitted; it is therefore difficult to establish a lower limit that works for all radionuclides. Therefore, volumes of 0.1, 0.5, 1.0, and 2.0 cm^3 for all three volumetric source geometries (i.e., cylinder, slab, and

sphere) were used to estimate dimensional quantities (e.g., radius, length, width, height) such that:

$$V_{slab} = r^3 \qquad V_{sphe} = \frac{4}{3}\pi r^3 \qquad V_{Cylinder} = \pi r^3$$

For example, a source with 1.0 cm^3 volume will have slab dimensions of 1.0 cm on all sides, a spherical radius of 0.62 cm, or a cylindrical length and radius both equal to 0.68 cm.

The user must supply source density in VARSKIN; this would be the density of material that houses the source activity, not necessarily the element of the radionuclide. The density can be difficult to determine depending on what is known about the source itself. We may know the precise activity, but the material in which the source is imbedded may be a mystery. This is especially true for small sources of some material that may be difficult to assess following a contamination event. As such, it is important to depict how dose responds to the density input with respect to source volume and geometry. For this analysis, density took on values of 0.5, 1.0, 2.0, and 4.0 g/cm^3. Additionally, model sensitivity to increasing area of a 2D disk source was determined. For both models, disk areas of 1.0, 2.5, 5.0, 7.5, 10, 15, and 20 cm^2 were simulated over a 10 cm^2 skin averaging area. The assumption was made that the VARSKIN user is aware of the activity present, but not as informed regarding the dimensions/make-up of the source.

To determine model sensitivities to airgaps and cover materials, a point source of nominal activity and varying energy was used for both the electron (0.01 – 8 MeV) and photon (0.001 – 3 MeV) model. Cover materials of 0.25, 0.5, 0.75, and 1.0 g/cm^3 with thicknesses of 0.2, 0.4, 0.6, 0.8, and 1 mm were simulated for both models. However, due to attenuation and energy-degradation differences, airgaps of 0.25, 0.5, 0.75, 1.0 *millimeters* and 0.25, 0.5, 0.75, 1.0 *centimeters* were simulated for the electron and photon models, respectively.

Our analysis of parameter (variable) sensitivity in the next two chapters is predicated on the following interpretation of data. Each plot shows the results for model calculations using inputs for different variables. The plot(s), taken individually or together, can reveal information as to the sensitivity of the output calculation for particular inputs. For example, Figure 1 shows simulated outputs for different input values of variables X, Y, and Z. Looking at a single line, the blue line in Figure 1a indicates that when Y=1 and Z=1 the model is most sensitive to variable X between values of 4 and 8 (the region of greatest slope). For multiple lines in a single plot, greater separation of those lines means greater model sensitivity to the variable differentiating the lines. So, looking at both lines of Figure 1a indicates that the model is not sensitive to changes in the value of Z when variable X has a value less than 4, yet thereafter sensitivity to variable Z increases

as X increases (greater separation of the green and blue lines as X gets larger). Additionally, a difference between two or more plots (looking at both Figures 1a and 1b) indicates output sensitivity to the input variable that differentiates the two plots (variable Y in this case). Thus, the two figures together provide evidence that the model is not sensitive to changes in Y for all values of Z (because the green and orange lines are essentially identical). However, the model is sensitive to the value of Y for values of Z when X has a value less than 3 (because the blue and purple lines are different below X = 3).

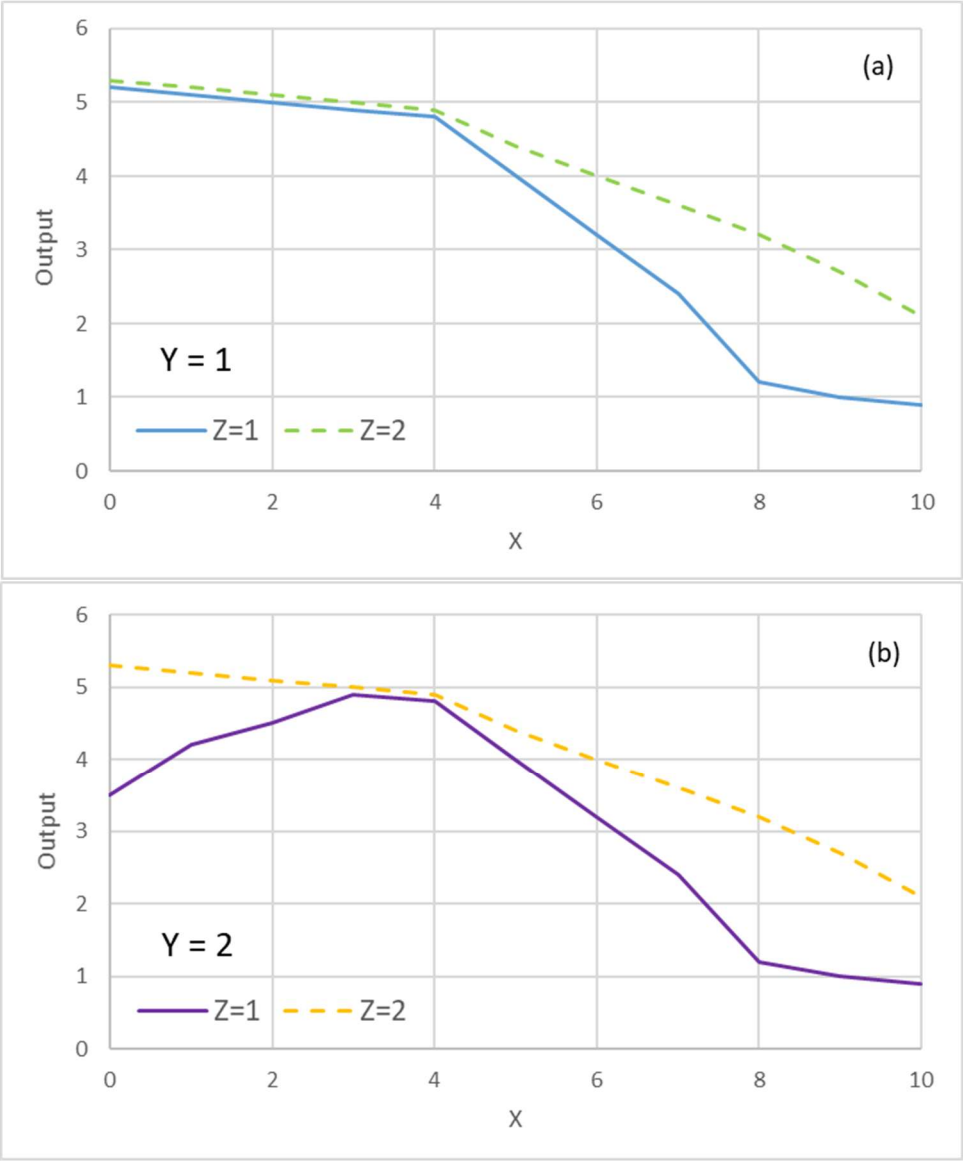

Figure 1: Examples of plots to describe interpretation techniques for determining parameter sensitivity.

5 Sensitivity in Electron Dosimetry

An important feature of electron energy loss is critical in assessing the influence of various parameters on shallow (7 mg/cm^2) skin dose. This feature relates to the change in stopping power of electrons as they travel through material and lose energy. The electron path through a medium does not follow a straight line and therefore complicates energy-loss patterns with skin depth (measured perpendicular to the surface). Figure 2 is a generalized plot of relative dose (i.e., dE/dx or stopping power) versus depth for electrons, photons, and protons. The plot suggests that maximum energy loss for electrons occurs at about 1/3 of the penetration depth.

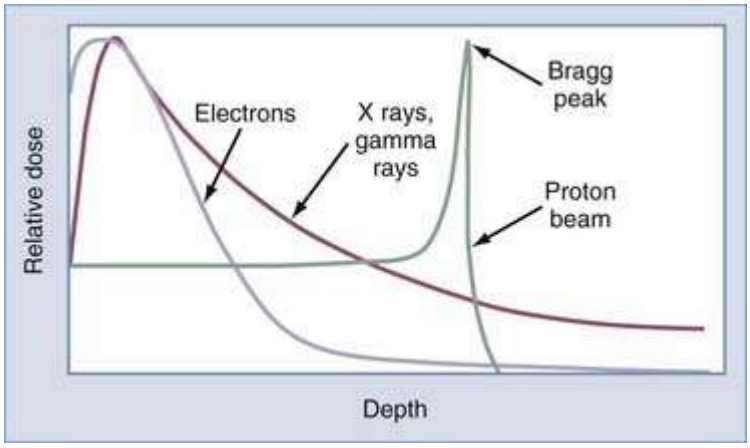

Figure 2: Stopping power (relative dose) as a function of depth for incident electrons, secondary electrons (from photons), and protons.

The shallow skin dose will have its greatest value if the depth of maximum relative dose (where we see electron peak dose in Fig. 2) happens to occur at a depth of 7 mg/cm^2. The position of that peak shifts to greater depth or lesser depth depending on what materials must be penetrated prior to reaching the skin. If, for example, the source is in a vacuum and no energy is lost prior to reaching skin, the relative dose peak will occur at its deepest depth. If, however, source and cover material are present between the emission point and the skin, the relative dose peak will occur at much shallower depths (and possibly even in the source or cover material before ever reaching the skin). Keeping this in mind, the reader will better understand how density and thickness of source and cover materials (and air gap) play a role in estimating electron dose at a specific depth in tissue.

In many of the plots that follow it is evident that an incident electron threshold energy of about 70 keV is necessary to reach a depth of 7 mg/cm^2, therefore dose rate is zero for energies less than the threshold.

5.1 Volumetric Sources

Volume, thickness and density of a three-dimensional source (or cover material) will affect the transport of electrons through that medium. As volume/density increases, so does the amount of material (i.e., number of atoms), and, due to Coulombic interactions between emitted electrons and the medium, source self-absorption is increased leading to greater electron energy loss prior to reaching the skin.

Figure 3 depicts the effect of changes in density and volume on the cylindrical volumetric source type (results for slabs and spheres are very similar and provided in the Appendix). We see that for each geometry, smaller source volumes result in higher skin dose simply due to less energy absorption in source material and the source generally being closer to the skin. Also, when the density is low, peak dose at the shallow depth occurs at lower monoenergetic electron energies (e.g., about 1 MeV). With each subsequent increase in source density, the peak dose occurs at higher electron energies since the electron loses more energy in the source and higher energy is required to reach even the shallow depth. Again, this is due to increased self-absorption and the reduction of the effective electron range in tissue. While the peak dose rate is also slightly shifted to higher energies at each specific density when volume is increased, the effect is not as significant. Additionally, it is evident that the peak dose at 1 MeV occurs between 0.5 and 1 g/cm^3 (for 0.1 cm^3 sources) due to a tradeoff between energy degradation and peak of the relative dose (stopping power) curve at 7 mg/cm^2. The model is shown to be moderately sensitive to electron energy more so for sources of smaller volume and lower density. Dose rate begins to register at about 90 keV in these plots, 20 keV higher due to the presence of source material. Each of the three geometries shows the same general trend.

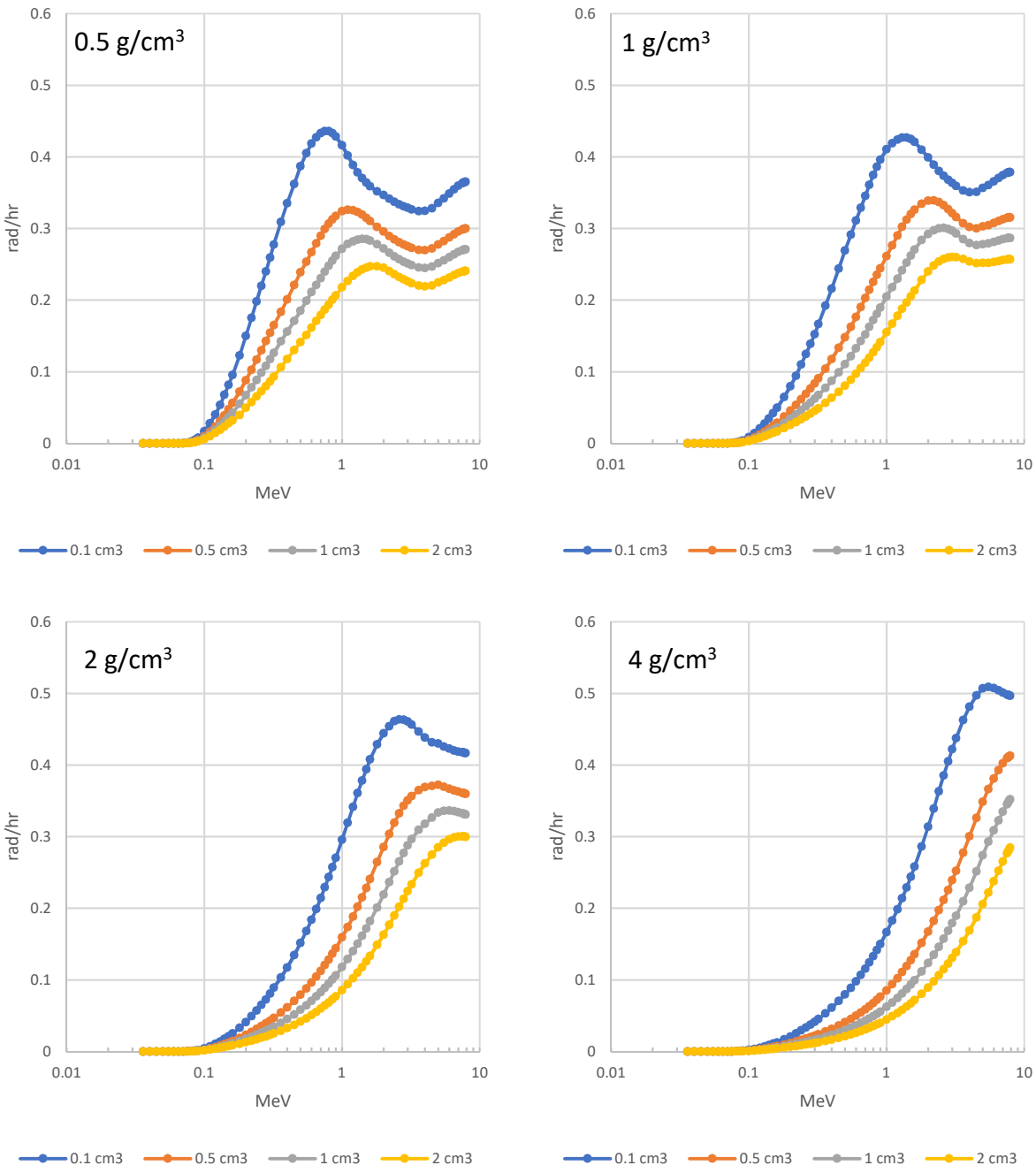

Figure 3: Electron dose rate for a cylindrical geometry as a function of energy and volume, by density.

Figure 4 depicts the deviation in dose rate (expressed as a percentage of dose rate for 1 cm^3 sources) at source densities of 0.5 and 2 g/cm^3 relative to 1 g/cm^3. These plots demonstrate the influence of electron energy and source density on dose rate. There is a dramatic change in percent deviation between electron energies of about 500 keV to 2 MeV. Cutting the source density in half (to 0.5 g/cm^3) will lead to an increase in dose at lower energies by about a factor of

2 since lower energy electrons may reach the end of their path length at the shallow dose averaging plane. However, the fraction of energy loss to higher energy electrons (> 2 MeV) is lower than those electrons traversing a 1 g/cm^3 source. As such, halving source density will lead to lower dose at higher electron energies (because the peak dose location is deeper than 7 mg/cm^2), with percent deviation tapering off at very high energy.

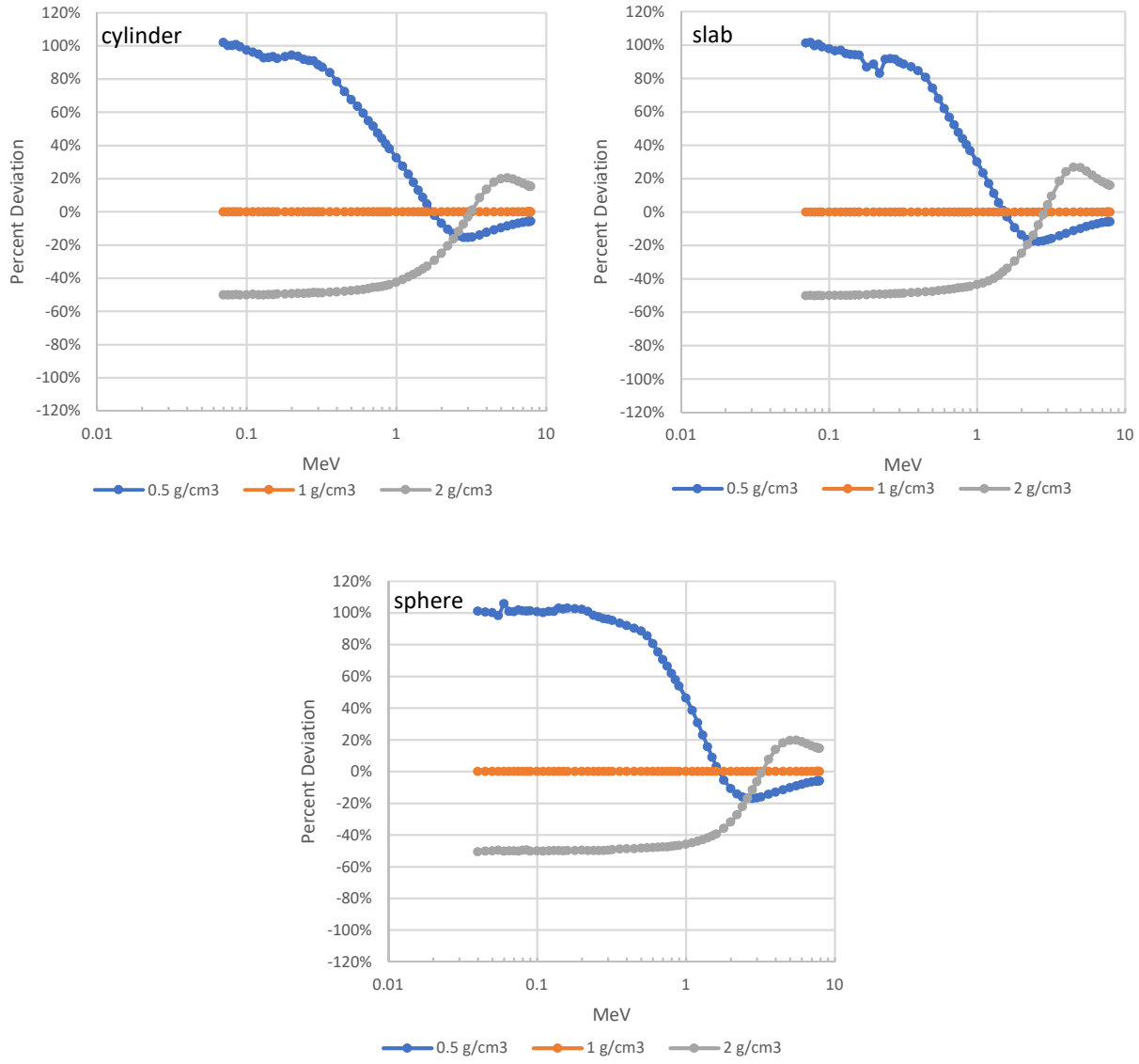

Figure 4: Electron dose variability for a 1 cm^3 volumetric source as a function of energy and density, by geometry.

The inverse occurs for doubling source density (to 2 g/cm^3). For energies less than 1 MeV a factor of 2 decrease in dose rate is observed. Further increasing the energy will lead to a 14-18% increase in dose rate at 7 MeV (see Table A1 in the Appendix). The effective range (and depth of peak dose) of lower energy electrons is reduced in comparison to the 1 g/cm^3 source, thus leading

to lower dose contribution. However, the opposite is true for higher energy electrons, leading to increased dose contribution. The plots of Figure 4 indicate that electron dose rate is more sensitive to variation in density for energies between about 200 keV and 2 MeV. The curves of Figure 4 (by geometry) all have the same general shape, except that of slabs at higher density where deviation peaks at about 4 MeV for the higher density source. *The VARSKIN user is cautioned to use an accurate density measure when invoking volumetric source geometries.*

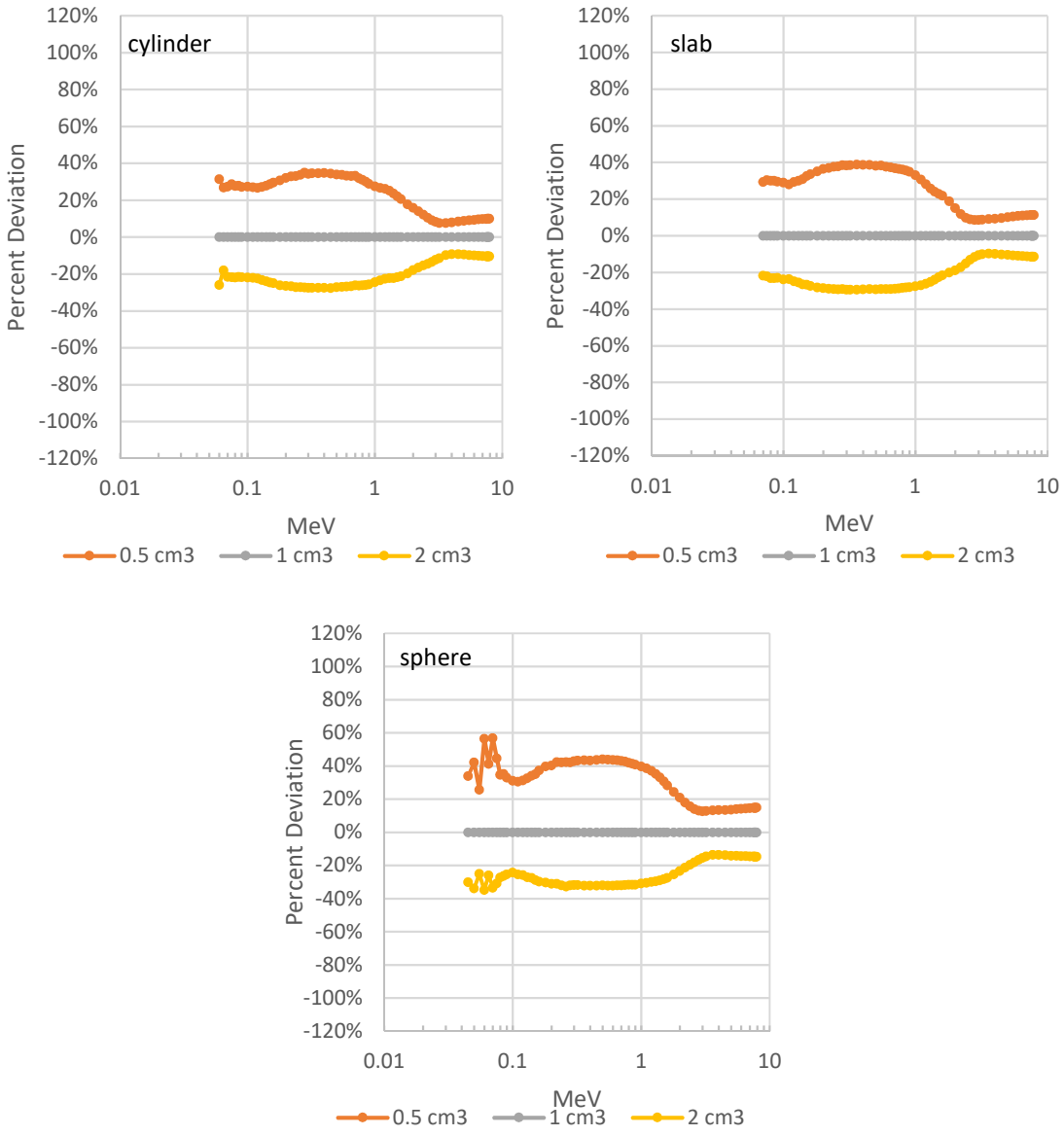

Figure 5: Electron dose variability for a 1 g/cm³ volumetric source as a function of energy and volume, by geometry.

Figure 5 (above) depicts the percent deviation of 1 g/cm³ sources for each volumetric geometry of 0.5 and 2 cm³ relative to 1 cm³ (same scale as Fig. 4). Up to 3 MeV there is a moderate

degree of variation from a 1 cm^3 source. Near 0.2 MeV, halving the source will lead to a 32-40% increase in dose whereas doubling will lead to a 26-31% reduction in dose (see Table A2). The difference gradually decreases with increasing energy to 10-15%, respectively. This variation at lower electron energies is primarily due to a slight increase in self-absorption with volume. However, as electron energy increases, self-absorption effects play less of a role in determining skin dose. Variability increases below about 3 MeV, with greatest sensitivity at very low energies and between about 1 and 3 MeV.

Figure 6a depicts the dose rate for 500 keV electrons from a slab volume as a function of density. For each volume, an increase in source density has a diminishing effect on dose. Similarly, Figure 6b provides the dose rate for each density as a function of volume. These plots demonstrate that variation in dose rate is largest at lower values of density and volume, as expected, with less sensitivity as volume and density increase. This is primarily due to internal source absorption approaching a state of "equilibrium" where only particles originating close to the source-tissue interface contribute to dose rate. As such, *accurate characterization of the source, especially for small volumes and low density, is crucial for electron dose estimation.* The same reduction in dose rate is observed for spherical and cylindrical sources, i.e., steeper curves (greater sensitivity) near low volumes and low density.

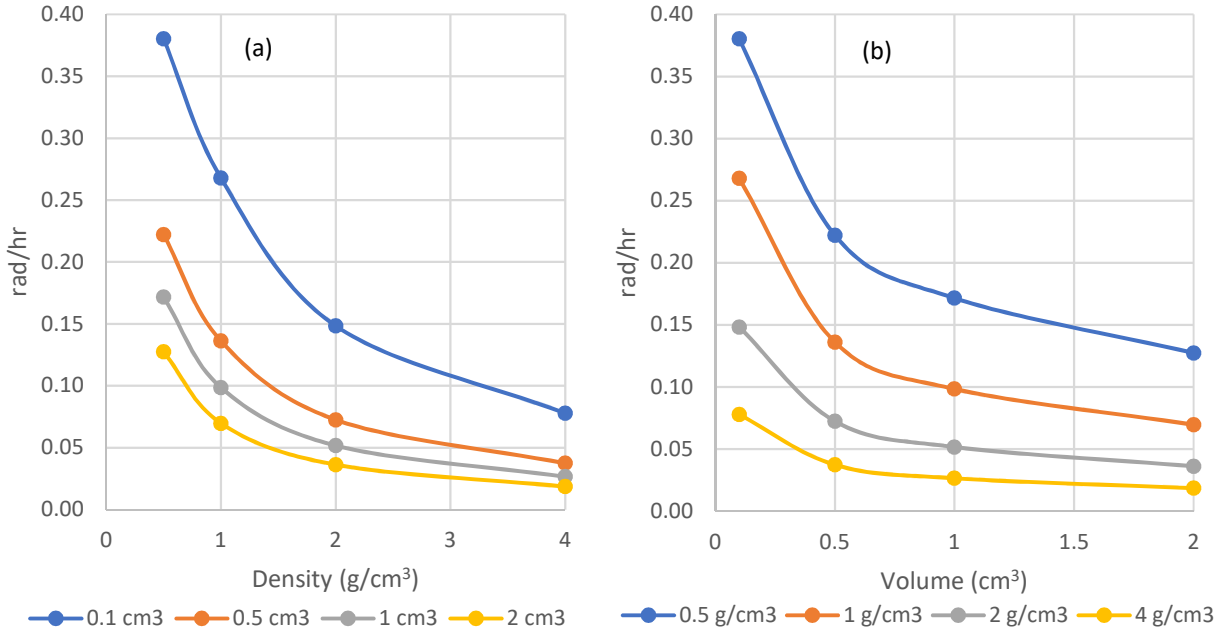

Figure 6: Dose rate for 500 keV electrons emanating from a slab as a function of (a) density over a range of volumes, and (b) volume over a range of densities. Note the dose rate scale is the same, but the x-axis represents different parameters.

5.2 2D Disk Sources

A two-dimensional disk source with surface area ranging from 1-20 cm², was simulated for electron dose estimates (Figure 7), assuming a 10 cm² skin dose averaging area at a depth of 7 mg/cm². Again, the dose rate is essentially zero for energies less than about 70 keV due to the short electron range and the small likelihood of low-energy electrons reaching the skin averaging area. Above an energy of about 120 keV, electrons are fully reaching the area and depositing maximum energy. There is then a decrease in dose rate up to an energy of about 1 MeV and a slight increase in dose rate as energy increases thereafter.

Above about 200 keV, as the area of the source increases for a constant source activity, dose rate decreases due to spreading of the source activity. This is especially pronounced at the boundary of the skin averaging area (10 cm²). When the source area surpasses 10 cm² dose rate drops considerably. Again, this is because the activity in the source is distributed over a larger area. This effect is more pronounced for electron dosimetry since the electron range in tissue is considerably short. When the area of the source is larger than the averaging area, much of the emitted electron energy is deposited in locations other than the 10 cm² averaging area.

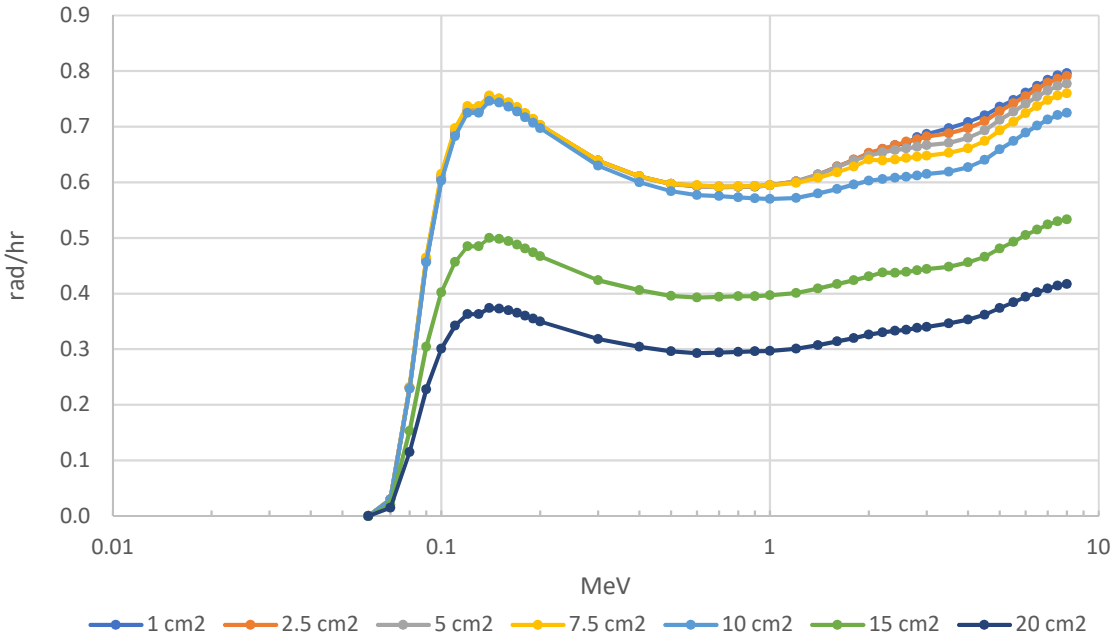

Figure 7: Electron dose rate for a 2-dimensional disk source as a function of energy and source area.

5.3 Cover Materials and Airgap

Cover material dimensions and densities of concern will have considerable effect on electron dose. With increasing thickness and density, the effective range of electrons within tissue will decrease significantly. Figure 8 depicts dose rate as a function of cover density and thickness. Sensitivity is greatest for lower energy electrons (100 to 500 keV) in low-density covers as they may be completely absorbed within the cover or in tissue prior to reaching the dose averaging plane. We see a similar result between 200 keV and 1 MeV for high-density covers. Like the results observed in the source geometry section, increasing cover material (either density or thickness) will lead to a general reduction in dose rate due to energy loss in that material. This is observed within each chart as the thickness of the cover material is increased. Additionally, as the density of the cover material increases, the effective range of electrons within tissue decreases. It is apparent that lower energy electrons may be completely absorbed before reaching the dose averaging plane. However, higher energy electrons will increase their dose contribution as a larger fraction of their energy is deposited at this point. If the cover (or source) removes the optimal amount of energy prior to reaching 7 mg/cm^2, the peak dose will occur.

Figure 9a depicts the percent deviation from a 0.4 mm thick cover when the cover density is halved or doubled relative to 0.5 g/cm^3. Dose is highly sensitive to low energy electrons less than 0.5 MeV when a cover is present. At this point the 0.25 g/cm^3 source delivers a dose rate 11.8% higher while the 1 g/cm^3 source is 20.7% lower (see Table A3). However, a cross-over occurs due to how electron range is affected at different densities. While halving the cover density allows lower energy electrons to reach the dose averaging plane, the fraction of energy loss for higher energy electrons will be lower than the 0.5 g/cm^3 case. As such, the 0.25 g/cm^3 cover will deliver lower dose rates at these higher energies with percent deviation tapering off to -4.4% at 7.5 MeV. Inversely, doubling the cover density will lead to increased absorption within the cover material at low electron energies thus leading to lower dose rates. This same phenomenon will cause an increase in dose rate for high energy electrons, with percent deviation leveling off at about 6.7%.

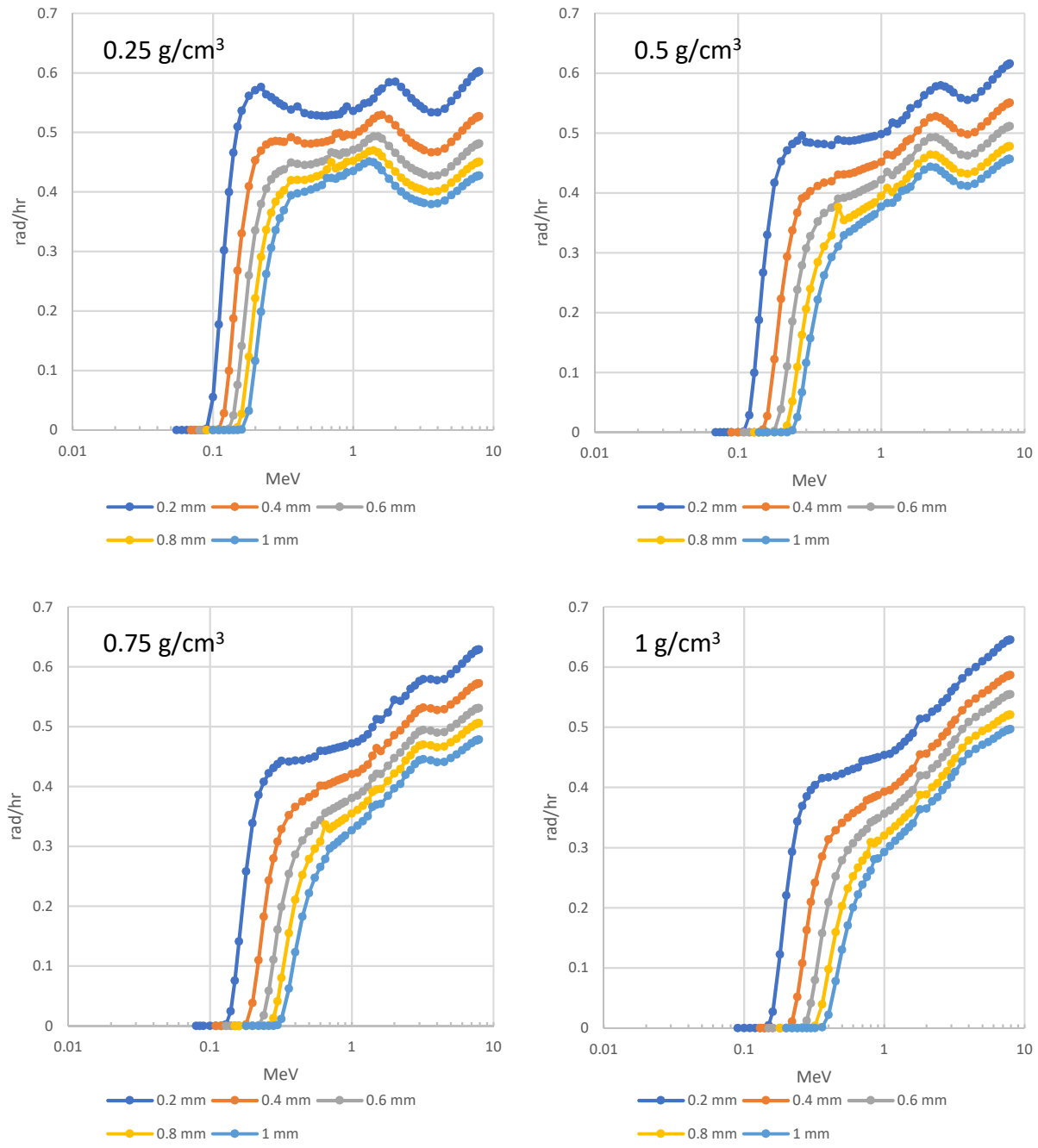

Figure 8: Electron dose rate for a point source on cover material as a function of energy and thickness, by density.

Figure 9b demonstrates the effect of doubling or halving cover thickness relative to a 0.4 mm thick cover with a density of 0.5 g/cm³. While there remain slight variations in range straggling, this effect is more prevalent at lower energies. Percent deviation begins to level off near 0.5 MeV indicating reduced sensitivity at higher energies. For the 0.2 mm cover, dose rates at this point are 13.6% higher than a 0.4 mm cover (see Table A4). Dose rates are 12.5% lower for

a 0.8 mm cover. The greatest sensitivity to cover material occurs when electron energy is less than about 0.7 MeV. These differences are like those observed in varying cover density. As such, the electron model is similarly sensitive to cover density and thickness.

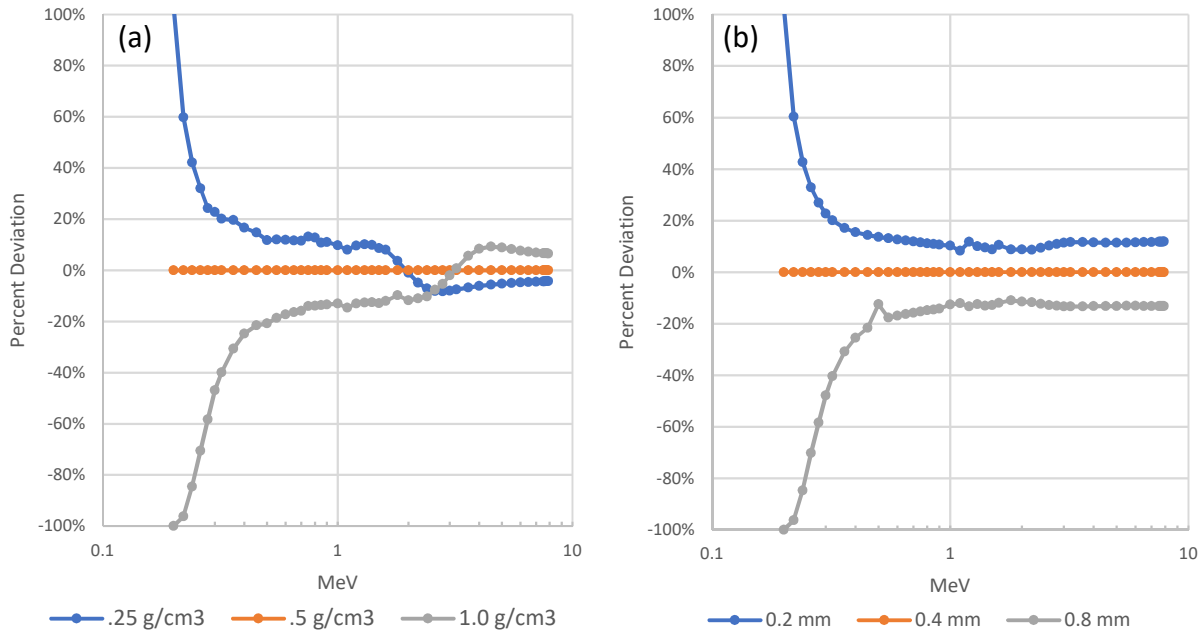

Figure 9: Electron dose variability as a function of energy for: (a) 0.4 mm cover thickness as a function of density and (b) 0.5 g/cm³ cover density as a function of thickness.

A further demonstration of electron model response to varying cover density and thickness is shown in Figure 10. Figure 10a depicts the change in dose rate for 500 keV electrons in each cover thickness as a function of cover density. Similarly, Figure 10b demonstrates the change in dose rate in each cover density as a function of cover thickness. The plots further suggest that the electron model is similarly sensitive to cover density and thickness inputs. This behavior is expected due to the use of density scaling (see Hamby et al. 2018) when determining equivalent water thicknesses for distances traversed by a particle in each layer.

Electron energy degradation in air is less pronounced than that for cover materials but is still present and slightly influential in the output dose rate (Figure 11). With an increase in airgap thickness, and above 0.4 MeV, dose rate decreases under geometric attenuation. A large portion of electron energy will be absorbed in air, leading to a significant dose reduction with increasing airgap thickness. Comparing Figure 9 to Figure 5, we see very similar results until about 500 keV. At that energy, the airgap begins to play a role in reducing dose rate with increasing airgap, likely due to energy degradation, geometric attenuation, and displacement of depth to reach peak dose.

The greatest sensitivity occurs for electrons above 500 keV so that *dose rate is more sensitive to the airgap for moderate to high energy electrons.*

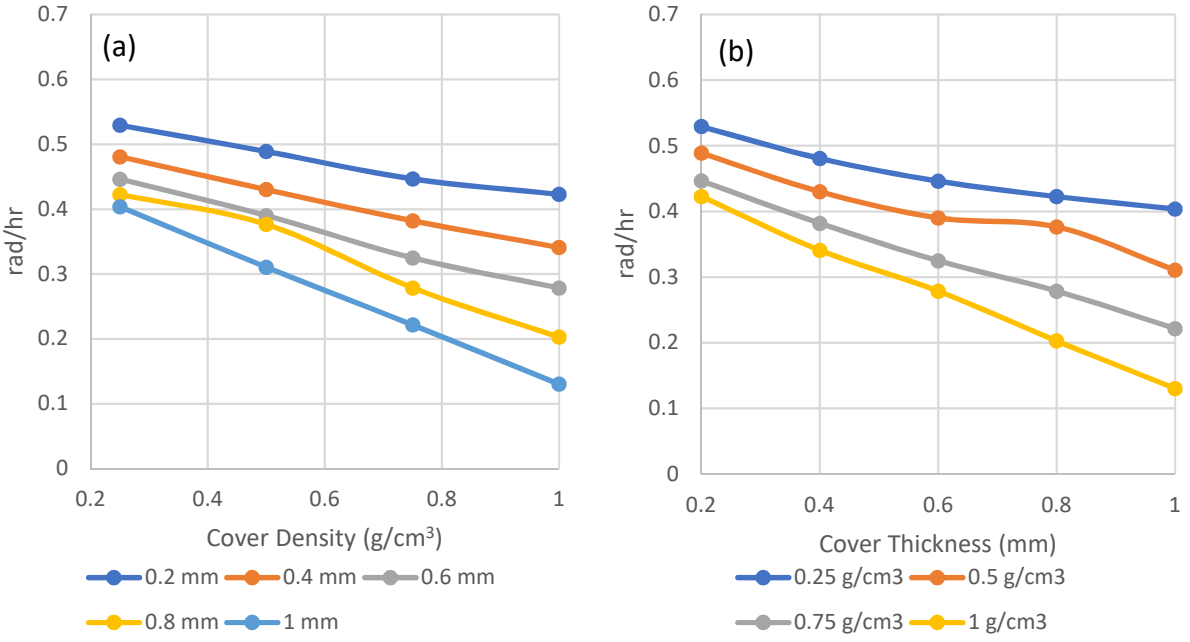

Figure 10: Dose rate for 500 keV electrons as a function of (a) cover density over a range of thicknesses and (b) cover thickness over a range of densities.

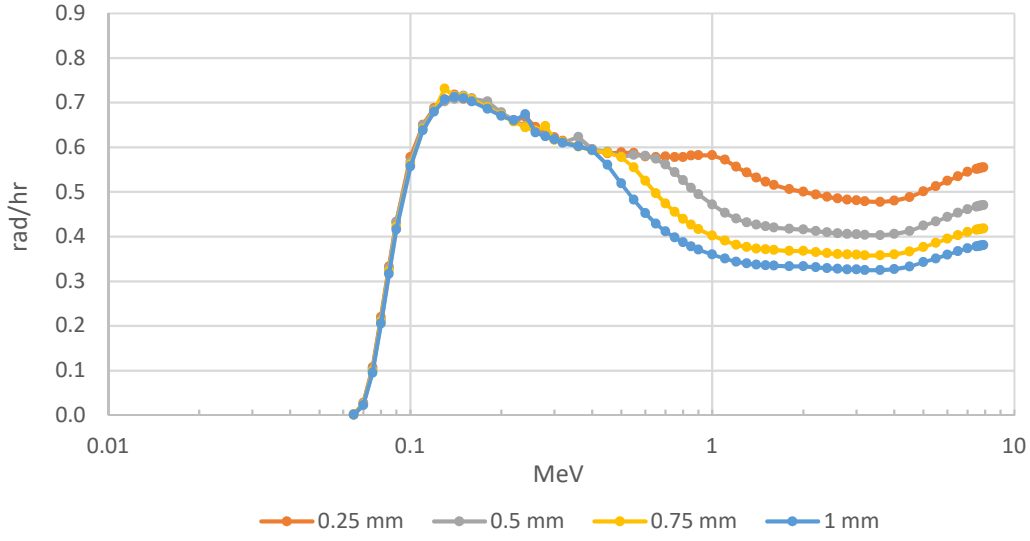

Figure 11: Electron dose rate for a point source as a function of energy and airgap distance.

6 Sensitivity in Photon Dosimetry

As with electrons, photon interactions also are characterized by a parameter that is helpful in our understanding of what influences shallow skin dose. In this case that parameter is the mass energy absorption coefficient (μ_{en}/ρ) which represents the probability of interaction as a function of material and photon energy. For example, Figure 12 provides an indication of the relative probability of photons depositing energy in water from 1 keV to 100 MeV.

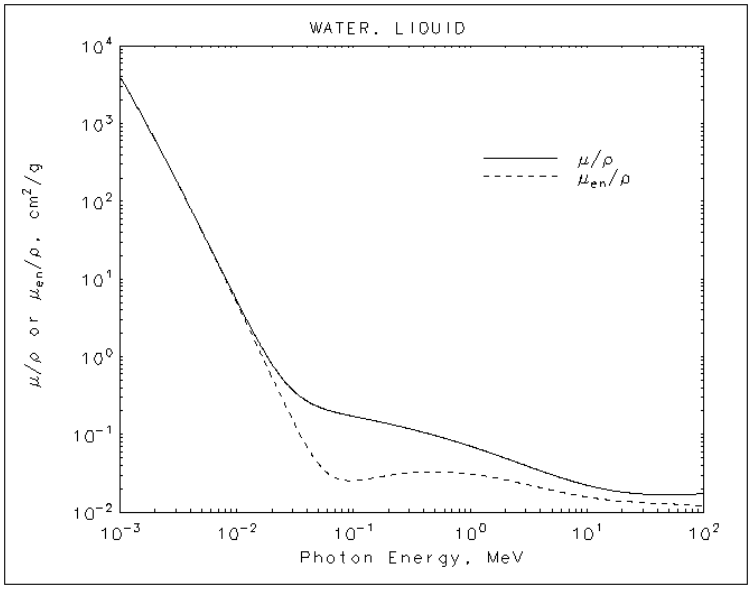

Figure 12: Mass energy absorption coefficient (μ_{en}/ρ) for photons interacting in water.

The plot of μ_{en}/ρ (dashed line) indicates that photons of energy below about 70 keV have increasingly higher probability of interaction as energy decreases, e.g., a 1 keV photon is more than 2 orders of magnitude more likely to deposit energy than a 10 keV photon. The plot also shows that for energies greater than about 70 keV, the probability of energy deposition is generally constant. The two major interaction mechanisms demonstrated in the plot are the photoelectric effect (lower energies) and Compton scatter (higher energies). The reader is encouraged to keep this interaction probability plot in mind while interpreting the photon sensitivity results.

Additionally, photons impinging on a material will liberate secondary electrons. Initially, the number of charged particles liberated in a volume of material will not be equal to the number of charge particles entering the same volume. Charged particle equilibrium (CPE) exists when the number and energy distribution of charged particles entering a mass of material is equivalent to the number leaving. For photons, this corresponds approximately to the range of secondary electrons. As such, the introduction of increasingly thick or dense source or cover material will

shift CPE to a shallower point within tissue or the cover itself. Lower energy photons that would have otherwise established CPE at the dose averaging plane will now reach this point at a shallower depth. Further attenuation of these photons and absorption of secondary electrons will lead to a lower dose contribution at the dose averaging plane. Similarly, higher energy photons will have a higher dose contribution due to establishment of CPE at the dose averaging plane when it would have otherwise been established at greater tissue depths.

6.1 Volumetric Sources

Material attenuation within the source, while considered in VARSKIN, is not significant in the photon model for several reasons. The effect of source attenuation is only a concern for large and dense sources well beyond the scope of VARSKIN. As such, it is assumed in the photon dose model that source material is equivalent to air for attenuation purposes (see Hamby et al. 2018).

Unlike electrons, photons of similar energy can travel considerable distances. Material attenuation within the source dimensions of concern (microns to centimeters) is negligible for energies greater than about 50 keV. However, geometric attenuation plays a more significant role as activity is distributed farther from the skin, but even this is relatively unimportant. While the source dimensions are such that the source is encompassed by the 10 cm^2 averaging plane, lateral source dimensions will have little effect. Vertical and horizontal dimensions will affect dose more dramatically due to geometric attenuation. The source dimensions of concern may not appear to be large, but their dimensions are several orders of magnitude greater than the tissue averaging depth of 70 microns.

Compared to the electron model, the variability in photon dose estimates between the three volumetric source geometries is less significant. As discussed, VARSKIN does not consider material attenuation within the source beyond that of air. While lateral dimensions displace activity over a larger portion of the dose averaging area, large variations in dose are not observed until these dimensions surpass the boundary of the dose averaging plane. For this analysis, all source dimensions of concern are encompassed within the 10 cm^2 plane such that the primary source of variation is an increase in the vertical dimensions of the source. The effect of lateral dimensions is further demonstrated in Section 6.2.

Under the assumptions for determining source dimensions from given volumes (see Section 4), there is a larger vertical spread for the sphere than any other source, ranging from 0.58-1.56 cm across all volumes. The cylinder has the smallest spread in vertical dimensions from 0.32-0.86 cm while the slab's vertical component ranges from 0.46-1.26 cm. Consequently, the cylinder and slab have less variation in dose rate with changing source volume than the sphere (Figure 13).

Density and volume of the source is not so important for photon dose model sensitivity. The plots show inflection points on the dose-rate curves at 6 keV and 70 keV. The inflection at 70 keV is due to the change in interaction mechanism explained above (see Figure 12), and the inflection at 6 keV occurs due to the depth of charged particle equilibrium coinciding with the dose averaging depth (7 mg/cm²). With two inflection points, sensitivity with energy is greatest in three different ranges. The dose rate sensitivity is low, however, for source volume.

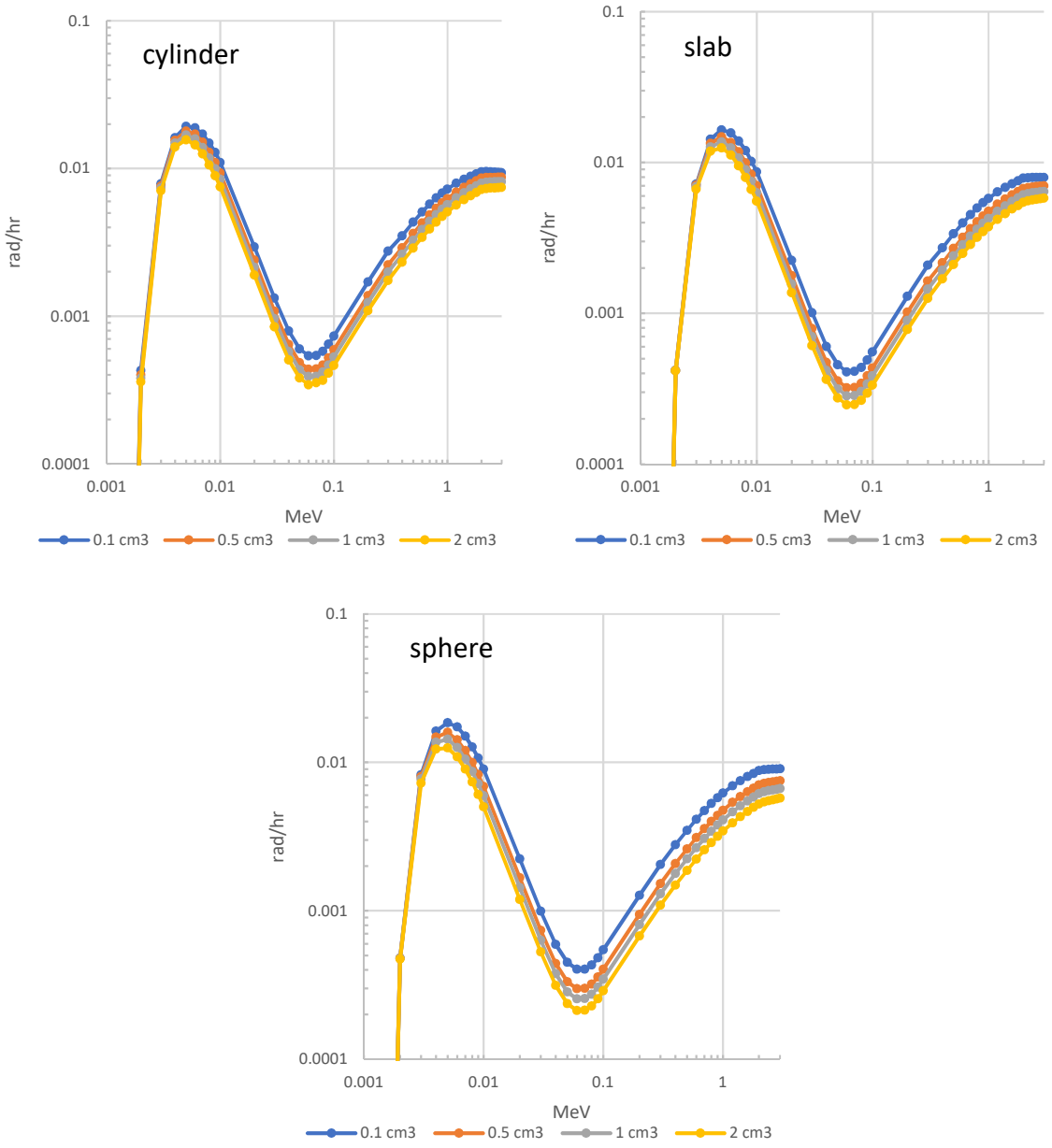

Figure 13: Photon dose rate as a function of energy and source volume, by geometry.

Figure 14 depicts the percent deviation for each geometry relative to a 1.0 cm^3 source when the source volume is either halved or doubled. Deviation is greatest for photons between 10 keV and 1 MeV, however, sensitivity to energy is greatest between about 2 and 10 keV. At 100 keV, the percent deviation from 1 cm^3 sources for 0.5 and 2.0 cm^3 is 12-17% higher and lower, respectively (see Table A5). Deviation remains near this level until near 1 MeV where it decreases to 8-14%. Greatest sensitivity to volume occurs at energies less than about 10 keV. The discontinuity occurring at 70 keV for 2 cm^3 slabs is under investigation.

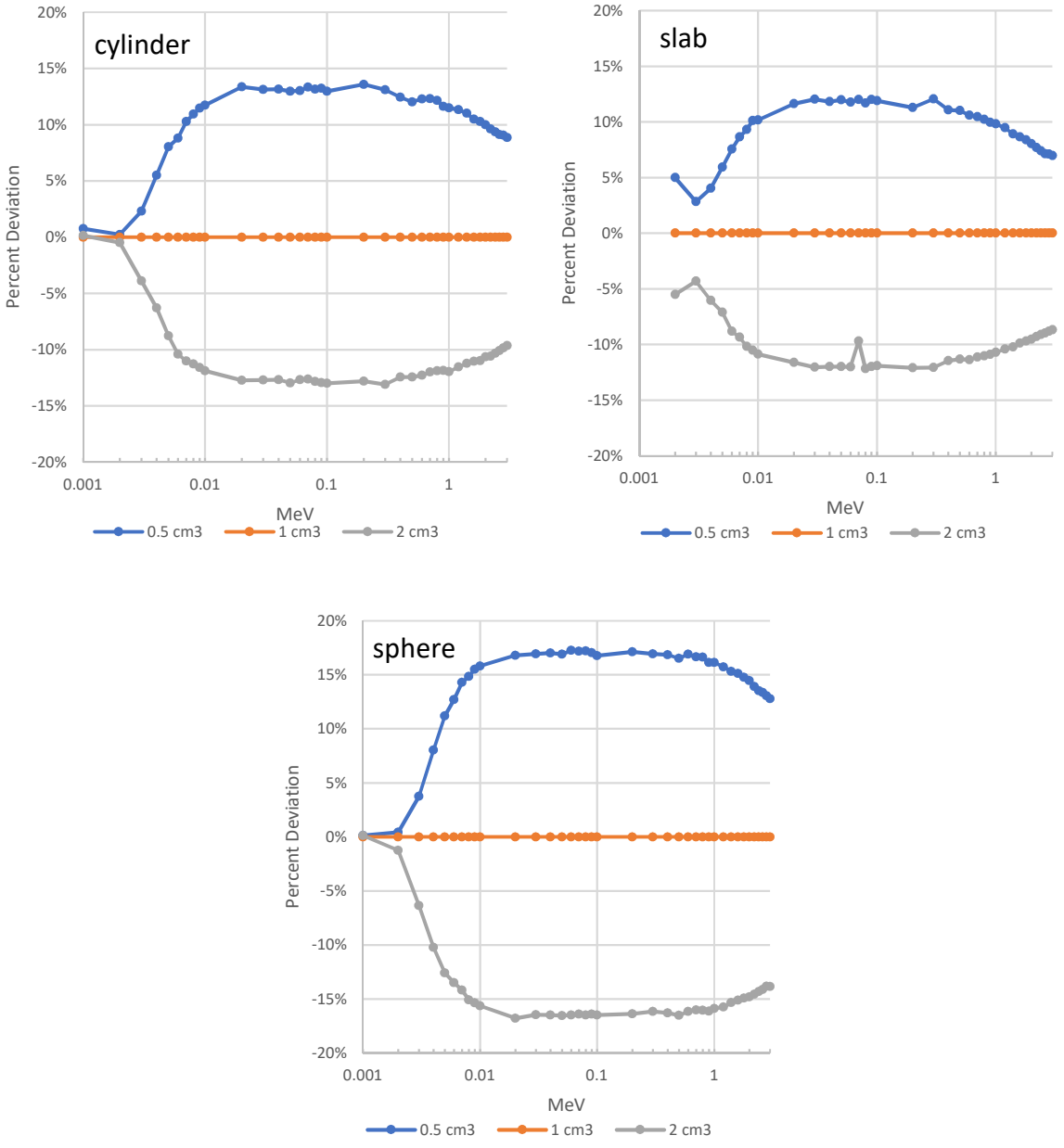

Figure 14: Photon dose variability as a function of energy and source volume, by geometry.

6.2 2D Disk Sources

A disk source with area ranging from 1-20 cm², was simulated for photon dosimetry (Figure 15). Dose is averaged over an area of 10 cm² for each simulation. As the area of the source increases, dose rate begins to drop because quanta will escape or will not fully deposit energy in the averaging area. This effect is more evident for electrons (due to their very short range), but photons show a reduced influence with source area. All curves fall on top of each other except for 15 cm² and 20 cm² when the source area is greater than the dose averaging area. The discontinuity in the curves of Figure 15 at 300 keV is due to a step function approach in the photon dose model. At 300 keV a function is introduced that accounts for high-angle scatter and electron loss through the surface of the skin (thus impacting CPE).

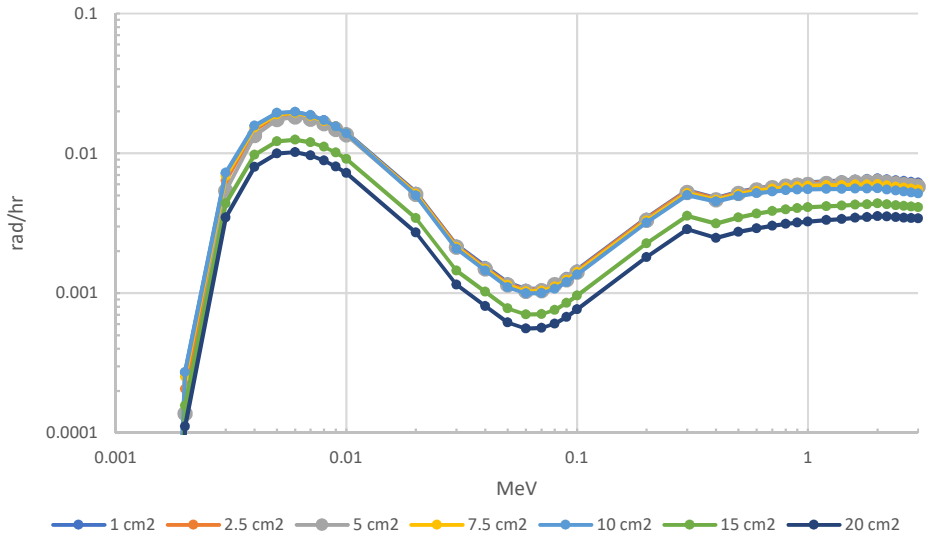

Figure 15: Photon dose rate for a 2-dimensional disk source as a function of energy and source area.

6.3 Cover Materials and Airgap

The dimensions and densities of cover materials were chosen to simulate common laboratory clothing items (lab coats, plastic gloves, cotton clothing, etc.). As previously discussed, the presence of a cover material will shift CPE to a shallower point within tissue for each specific photon energy. Under the dimensions simulated, increases in cover thickness will lead to higher dose rates for high energy photons (Figure 16). This is due to the same phenomena, allowing for CPE to be established near the dose averaging plane where, in the absence of a cover, CPE would be established past this point. The tradeoff between establishing CPE before and after the dose plane is demonstrated for each plot with increasing energy. For energies greater than 1 MeV,

larger covers yield higher dose rates due to this effect. *Generally, photon dose is not sensitive to cover characteristics with very little difference in dose rate to changes in density and volume.*

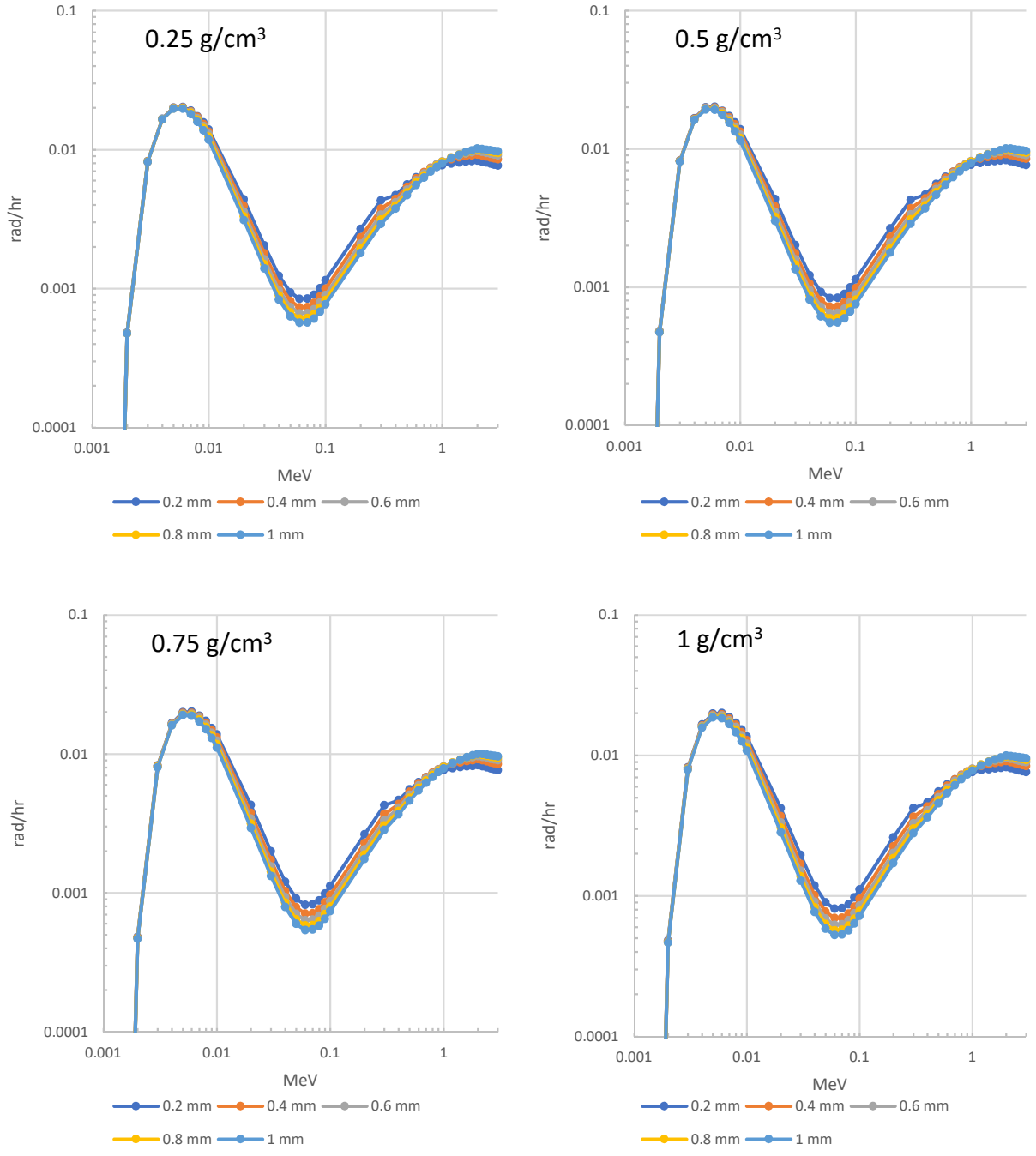

Figure 16: Photon dose rate for a point source as a function of energy and cover thickness, by density.

For cover material thicknesses and densities like that of common clothing items, the photon model yields the following. Depicted in Figure 17a is the percent deviation for 0.4 mm covers of 1 or 0.25 g/cm³ relative to 0.5 g/cm³. The effect of doubling the cover density shows that there will

be, at most, a 4.7% reduction in dose (see Table A6). Halving the cover density will yield a 2% increase in dose. The largest variation occurs at low energies (10 to 500 keV). As energy increases, these differences gradually level off at approximately 1% and 1.3%, respectively. *The photon model is not sensitive to cover density.*

Figure 17b depicts the percent deviation for 0.5 g cm^{-3} covers of 0.2 or 0.8 mm relative to 0.4 mm. This plot further demonstrates the phenomena of CPE being established before and after the dose plane. There is a sharp increase in the deviation from 5 to 30 keV, and again from 300 keV to 2 MeV. At 100 keV, a 16-18% deviation occurs from either halving or doubling thickness (see Table A7). The smaller cover thickness will yield larger doses until 0.7 MeV and the larger cover thickness will yield smaller doses until 1 MeV. Above 300 keV sensitivity to photon energy is high. From 1-3 MeV, the differences will gradually increase to 10-11% for both comparisons. *The photon model is more sensitive to variation in cover thickness than in cover density.*

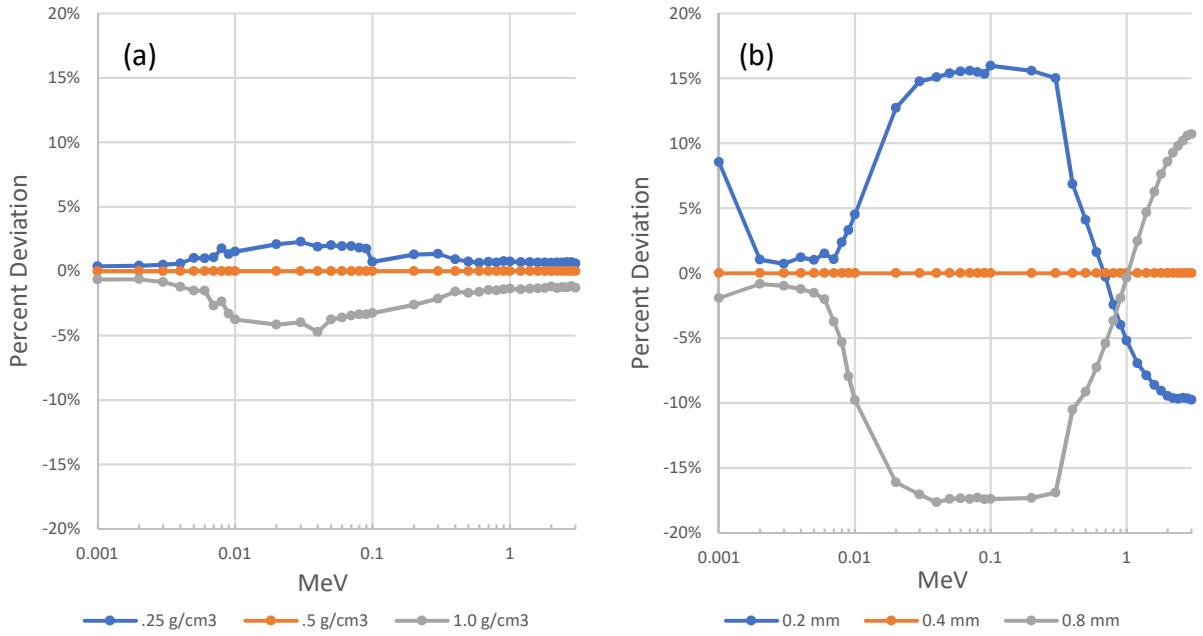

Figure 17: Photon dose variability as a function of energy for a (a) cover of 0.4 mm thickness with varying density and a (b) cover of 0.5 g/cm³ density with varying thickness.

Figure 18 further depicts that the photon model is most sensitive to cover thickness and minimally sensitive to cover density. Figure 18a shows the variation in dose for each cover thickness with changing density. For photons, with each subsequent increase in cover density, dose rate is only slightly affected. Figure 18b depicts variation with changing cover thickness. As previously discussed, the output demonstrates a higher sensitivity to cover thickness with the variation in dose rate being more pronounced.

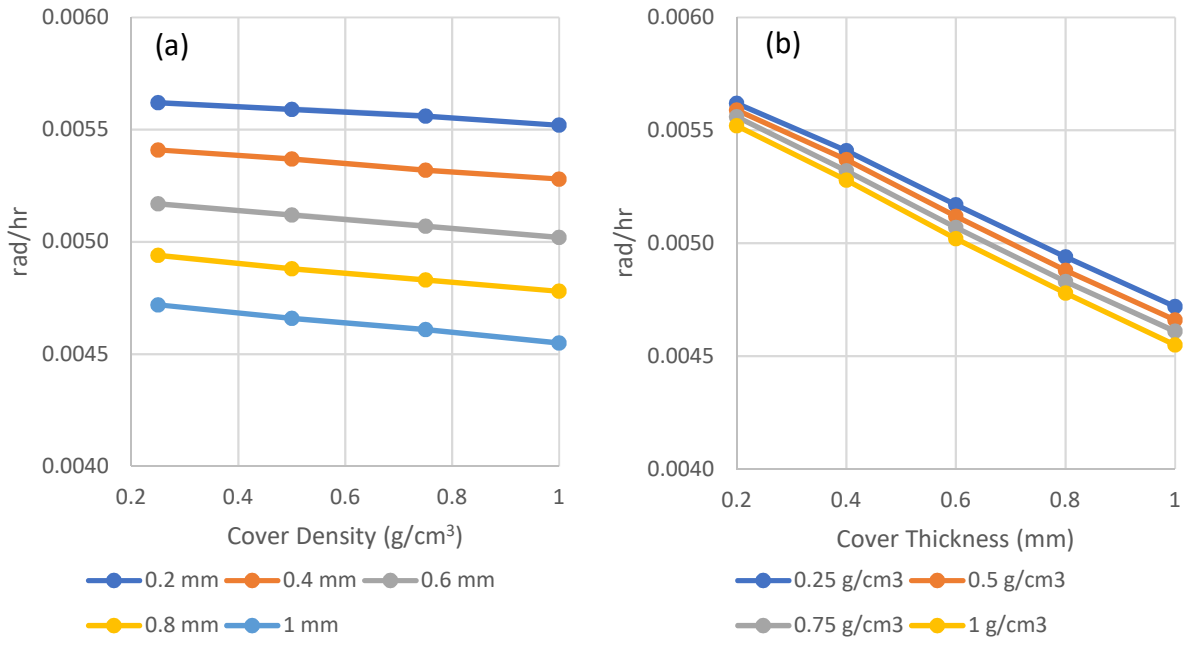

Figure 18: Dose rate for 500 keV photons as a function of (a) cover density over a range of thicknesses and (b) cover thickness over a range of densities.

The photon dose model is more sensitive to material attenuation in air than that for cover materials (Figure 19). For the photon model, geometric attenuation from a point source drives the reduction in dose rate. This is demonstrated through increasing airgaps of 0.25-1 cm. With each subsequent increase in airgap thickness, dose at each energy level decreases under geometric attenuation. When comparing Figure 19 to Figure 16, *airgap thickness appears to be more important than both cover density and thickness*. Again, geometric attenuation is the primary source of dose rate sensitivity in the photon model.

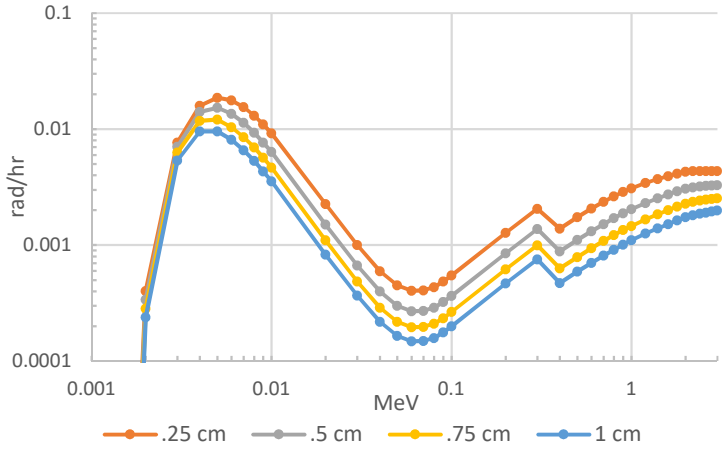

Figure 19: Photon dose rate for a point source as a function of energy and airgap.

7 Summary

As stated earlier, user analysis of a contamination event is the single largest source of uncertainty in VARSKIN. The electron and photon models respond differently to a variety of factors that the user must define when analyzing a skin-contamination event. Electron and photon models both rely on accurate information to account for all physical effects in radiation transport. Although improvement of the models employed by VARSKIN will continue, it is difficult to account for inherent uncertainty in human interpretation.

The parameters that are direct propagators of uncertainty (exposure time, activity, and distributed activity) will always be 1-for-1 in terms of output sensitivity to the input parameter. During typical use of VARSKIN, most of the dose sensitivity lies in these direct multipliers. The inputs without parametric uncertainty (volume averaging depth, skin averaging area, and skin thickness), because they are defined by regulation (e.g., dose averaged over 10 cm^2 at a depth of 7 mg/cm^2), will provide zero uncertainty to the dose calculations due to their mandated use.

The remaining parameters are those with parametric uncertainty, and therefore have been the focus of this report. Recall, the parameters of source diameter, thickness, and X- and Y-dimensions for volumetric sources were combined into an examination of dose sensitivity to "source volume". If the direct multipliers are well known, the influence of source material, cover material, and airgap provide the next level of importance to parametric sensitivity.

Generally, variations in dose can be attributed to how user input affects material and geometric attenuation. The user must define the characteristics such as density and volume for both the source and cover material. For the electron model, slight variations in these parameters can lead to significant differences in dose, especially at lower electron energies. This is due to a particularly sensitive dose response to material absorption of electron energy, whether in the cover or source itself. The dose response to photons is not as drastic, but non-trivial deviation in dose is still observed for variation in source and cover characteristics.

Table 1 summarizes the sensitivity of the electron dose calculation to its appropriate inputs. In general, electron dose is not sensitive to geometry type, yet is shown to be moderately sensitive to lower electron energies more so for sources of smaller volume and lower density. Electron dose appears to be more sensitive to variation in source density for energies between about 200 keV and 2 MeV. Dose rate is shown to be sensitivity to source volume at very low electron energies and those between about 1 and 3 MeV. We have demonstrated that dose rate sensitivity is largest at lower values of density and volume, with decreasing sensitivity as volume and density increase.

When the 2D source area is greater than 10 cm^2 (the mandated averaging area) dose rate drops considerably. The greatest sensitivity to cover material occurs when electron energy is less than about 700 keV, with reduced sensitivity at higher energies. The electron model is similarly sensitive to cover density and thickness since both parameters impact electron energy degradation prior to reaching the skin. The greatest sensitivity to airgap thickness occurs for electrons above 500 keV; below that energy, airgap seems to have no impact on electron dose.

Table 1. Sensitivity of the electron dose model to the listed parameters.

Parameter	E < 200 keV	200 keV – 2 MeV	E > 2 MeV
3D Geometry	LOW	LOW	LOW
3D Source volume*	HIGH	HIGH/MODERATE	MODERATE
3D Source density**	HIGH	HIGH/MODERATE	MODERATE
2D Source area*** (relative to avg area)	LOW	LOW/MODERATE	LOW/MODERATE
Cover density	MODERATE	MODERATE	LOW
Cover thickness	HIGH	LOW	LOW
Airgap thickness	LOW	MODERATE	MODERATE

*HIGH/MODERATE signifies high sensitivity for sources of lower volume and moderate sensitivity for higher volume.

**HIGH/MODERATE signifies high sensitivity for sources of lower density and moderate sensitivity for higher density.

***LOW/MODERATE signifies low sensitivity for source area less than the dose averaging area and moderate sensitivity for source area greater than the dose averaging area.

Table 2 summarizes the sensitivity of the photon dose calculation to its appropriate inputs. In general, the choice of geometry type and attenuation caused by the source is not significant in the photon model (therefore, air is assumed). Material attenuation within the source dimensions of concern (microns to centimeters) is negligible for energies greater than about 50 keV. The variability in photon dose estimates between the three volumetric source geometries is less significant than for electrons. The cylinder and slab have less variation in dose rate with changing source volume than the sphere due to an increase in the physical displacement of source to skin. Model sensitivity to source density and volume is low, with sensitivity to volume being greatest between photon energies of about 2 and 10 keV. The size of the two-dimensional disk source has essentially no impact on dose, as long as it is smaller than dose averaging area. Generally, photon dose is not sensitive to cover characteristics, with very little difference in dose rate to changes in

density and volume. Above 300 keV, however, dose sensitivity to cover thickness is increased. Airgap thickness appears to be more important than both cover density and thickness.

Table 2. Sensitivity of the photon dose model to the listed parameters.

Parameter	E < 20 keV	20 keV - 500 keV	E > 500 keV
3D Geometry	LOW	LOW	LOW
3D Source volume	MODERATE	LOW	LOW
3D Source density (assumed to be air)	LOW	LOW	LOW
2D Source area*	LOW	LOW/MODERATE	LOW/MODERATE
Cover density	LOW	LOW	LOW
Cover thickness	LOW	MODERATE	MODERATE
Airgap thickness	LOW	MODERATE	MODERATE

***LOW/MODERATE signifies low sensitivity for source area less than the dose averaging area and moderate sensitivity for source area greater than the dose averaging area.

All in all, the VARSKIN user is cautioned to use an accurate density measure when invoking volumetric source geometries for electron dosimetry. As such, accurate source characterization, especially for small volumes and low density, is crucial for electron dose estimation. The photon model is more sensitive to variations in cover and airgap thickness (likely due to geometric attenuation) than in cover density.

8 References

Anspach, L.J.; Hamby, D.M. Performance of the VARSKIN 5 (v5.3) Electron Dosimetry Model. *Radiation Protection Dosimetry*. 181(2):111-119. October 2018.

Dubeau, J., Hakmana Witharana, S.S., Sun, J., Heinmiller, B.E., Chase, W.J. A Comparison of Beta Skin Doses Calculated with VARSKIN 5.3 and MCNP5. *Radiation Protection Dosimetry*. 182(4):502-507. December 2018.

Hamby, D.M., Mangini, C.D., Caffrey, J.A., Tang, M. "VARSKIN 6: A Computer Code for Skin Contamination Dosimetry." NUREG/CR-6918, Rev 3. Washington, DC: U.S. Nuclear Regulatory Commission. 2018.

Mangini, C.D. "Beta-particle backscatter factors and energy-absorption scaling factors for use with dose-point kernels." Doctoral Dissertation. Oregon State University. December 2012.

9 Appendix

Listing of similar plots and tabulations

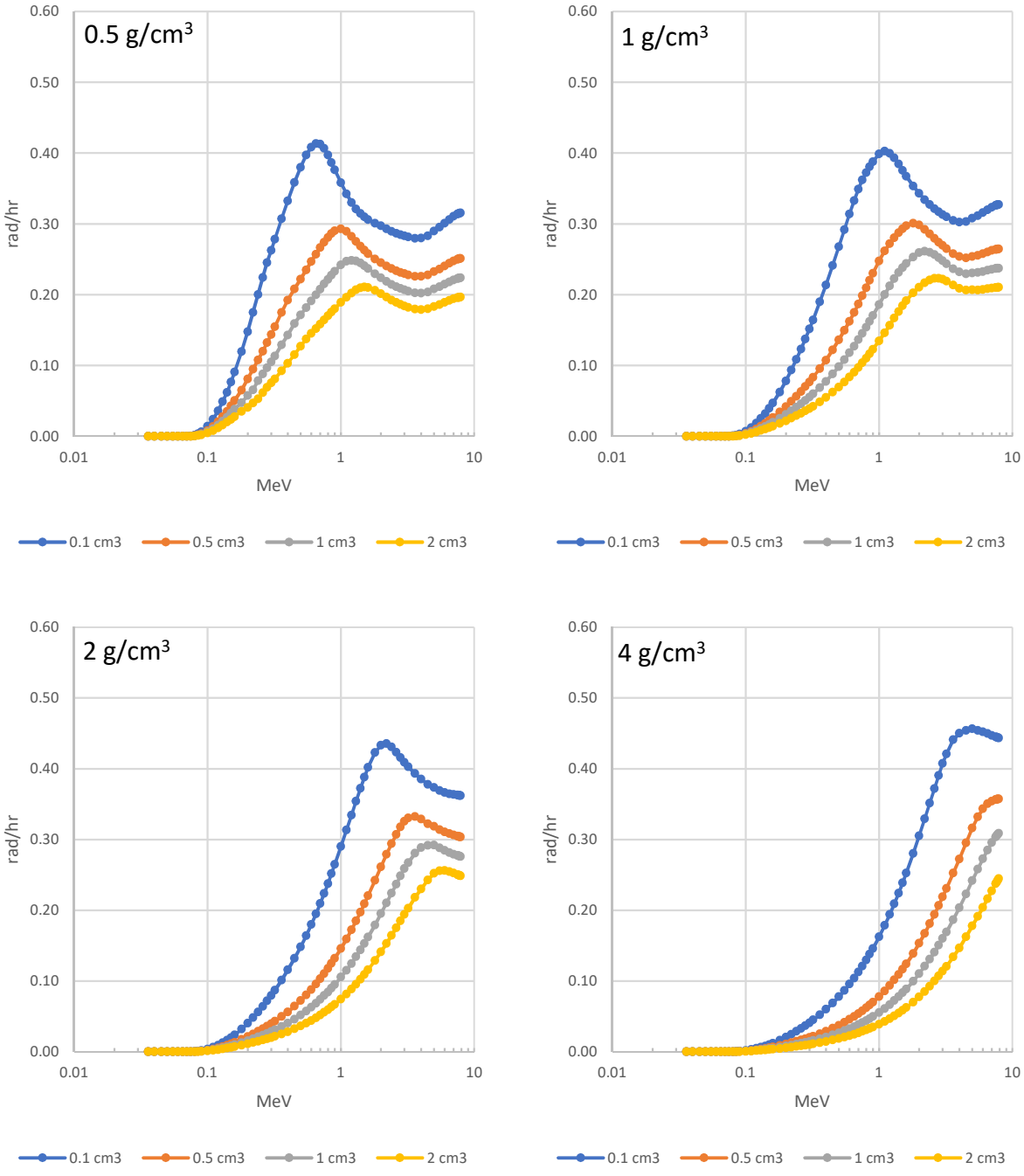

Figure A1: Electron dose rate for a slab geometry as a function of energy and volume, by density.

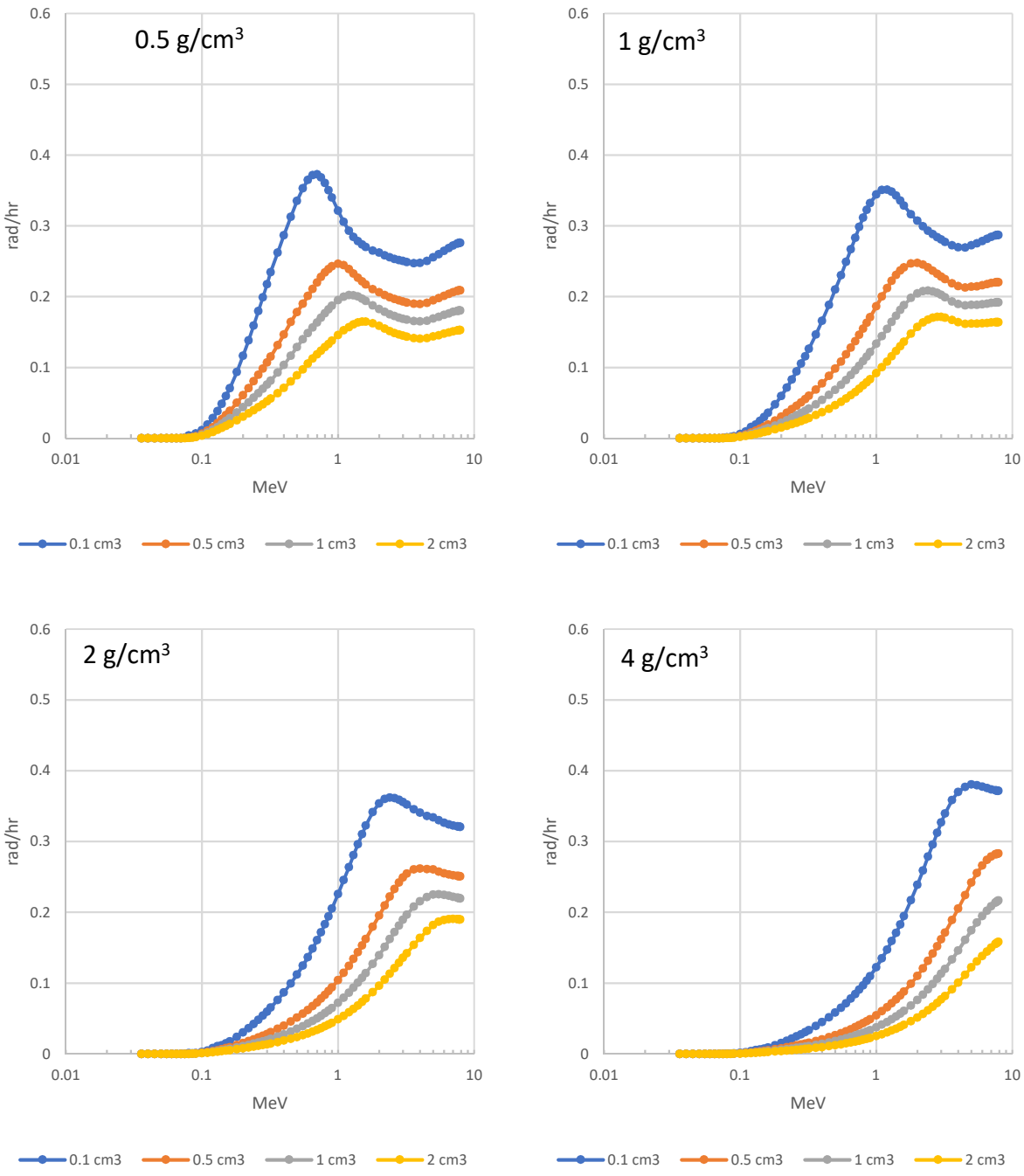

Figure A2: Electron dose rate for a spherical geometry as a function of energy and volume, by density.

Table A1: Percent deviation from 1 g/cm³ source.

Energy (MeV)	Percent Deviation from 1.0 g/cm³ (%)					
	0.5 g/cm³			2 g/cm³		
	Sphere	Slab	Cylinder	Sphere	Slab	Cylinder
0.2	102	88.5	94.5	-49.6	-49.2	-49.2
0.4	92	84.6	78.5	-48.7	-48	-48.2
0.6	80.6	61.9	59.5	-48	-46.7	-46.6
0.8	61.8	44	44.2	-47.2	-45.2	-44.9
1	46.3	30.1	32.7	-45.9	-43.4	-42.5
2	-10.7	-13.7	-6.9	-31.8	-24.7	-25
3	-16.6	-16.6	-15.4	-6.3	-4.3	-3
4	-13	-12.8	-12.4	13.8	24.2	13.7
5	-10.2	-9.9	-9.6	19.6	26.6	20
6	-8.1	-7.7	-7.5	18.7	22.1	19.8
7	-6.6	-6.4	-6.3	14.8	18.2	17.3

Table A2: Percent deviation from 1 cm³ electron source

Energy (MeV)	Percent Deviation from 1.0 cm³ (%)					
	0.5 cm³			2 cm³		
	Sphere	Slab	Cylinder	Sphere	Slab	Cylinder
0.20	40.4	36.6	32.1	-31	-28.5	-26.4
0.40	43.3	38.8	34.9	-32.1	-29.2	-27.4
0.60	43.7	37.7	33.3	-32.1	-29	-26.7
0.80	42.1	36.2	31.1	-31.7	-28.3	-26
1	39.8	33.1	27.5	-30.9	-27.5	-24.4
1.2	37.2	28.2	26.3	-30	-26.1	-22.5
1.4	33.3	24.1	23.8	-28.9	-23.9	-22.1
1.6	28.4	21.9	20.7	-27.5	-21.5	-21.2
1.8	24.5	18.8	17.8	-25.5	-19.9	-19.6
2	21.1	15.1	16	-23.2	-18.8	-17.9

Table A1: Percent deviation for electron point source with varying cover density from 0.4 mm cover with a density of 0.5 g/cm³

Energy (MeV)	Percent Deviation from 0.4 mm Cover with 0.5 g/cm³ (%)	
	0.25 g/cm³	1.0 g/cm³
0.2	103	-100
0.5	11.8	-20.7
1.0	9.8	-13.0
1.5	3.6	-12.9
2.0	-1	-11.8
3.0	-8	-2
5.0	-5.3	8.8
7.5	-4.4	6.7

Table A2: Percent deviation for electron point source with varying cover thickness from 0.4 mm cover with a density of 0.5 g/cm³

Energy (MeV)	Percent Deviation 0.4 mm Cover with 0.5 g/cm³ (%)	
	0.2 mm	0.8 mm
0.2	103	-100
0.5	13.6	-12.5
1.0	10.2	-12.5
1.5	8.8	-12.8
2.0	8.8	-11.5
3.0	11.4	-13.4
5.0	11.4	-13.1
7.5	11.8	-13.2

Table A3: Percent deviation from 1 cm³ photon source

Energy (MeV)	Percent Deviation from 1 cm³ (%)					
	0.5 cm³			2 cm³		
	Sphere	Slab	Cylinder	Sphere	Slab	Cylinder
0.1	16.8	13.0	11.9	-16.5	-13.0	-11.9
0.5	16.5	12.0	11.0	-16.5	-12.4	-11.3
1.0	16.1	11.5	9.8	-15.9	-12.0	-10.7
2.0	14.5	10.0	8.0	-14.8	-10.6	-9.5
3.0	12.8	8.6	7.0	-13.8	-9.6	-8.7

Table A4: Percent deviation for photon point source with varying cover density from 0.4 mm cover with a density of 0.5 g/cm³

Energy (MeV)	Percent Deviation from 0.4 mm Cover with 0.5 g/cm³ (%)	
	0.25 g/cm³	1.0 g/cm³
0.04	1.89	-4.72
0.5	0.75	-1.68
1.0	0.74	-1.36
2.0	0.65	-1.20
3.0	0.59	-1.29

Table A5: Percent deviation for photon point source with varying cover thickness from 0.4 mm cover with a density of 0.5 g/cm³

Energy (MeV)	Percent Deviation from 0.4 mm Cover with 0.5 g/cm³ (%)	
	0.2 mm	0.8 mm
0.1	16.0	-17.4
0.5	4.1	-9.1
1.0	-5.2	-0.4
2.0	-9.5	8.6
3.0	-9.7	10.7